Journal of Marine Research, 68, 503–522, 2010

On the variability of Gulf Stream transport from seasonal to decadal timescales

by T. Rossby[1,2], C. Flagg[3] and K. Donohue[1]

ABSTRACT

Given the Gulf Stream's central role in the North Atlantic's wind-driven and meridional overturning circulation (MOC), there is considerable interest in measuring mass and heat flux to sufficient accuracy that their variability can be quantified with some degree of confidence. Here we combine high-resolution direct measurements of upper ocean transport from the last 17 years of Oleander ADCP data with previously published estimates of baroclinic transport to examine Gulf Stream transport variability over the last 80 years just downstream of where the current separates from the U.S. east coast.

By far the greatest source of variability occurs on short time scales related to the meandering of the current and energetic eddy field to either side such that the inherent uncertainty of a single transport estimate is ~15% with respect to an annual mean. The annual cycle of layer transport at 55-m depth has a maximum increase of 4.3% of the mean in September while the annual cycle at 205 m reaches a maximum of only 1.5% in July. A running low-pass filter indicates transport variations of only a few percent of the mean on inter-annual and longer time scales although swings as large as 10–12% over a few years can occur. The length of the time series now reveals a significant correlation between the NAO index and near-surface transport in the Gulf Stream. No significant trend in transport can be detected from either the last 17 years of directly measured surface currents, or from hydrographic sections starting in the 1930's. It follows therefore that the upper branch of the MOC, the other major component of Gulf Stream transport at the Oleander line, must have been quite stable over the last 80 years.

1. Introduction

Numerous efforts have been made over the years to determine Gulf Stream (GS) transport off the U.S. east coast. The task would seem straightforward given that one cannot fail to cross it, and almost always it exhibits an easily recognized shape. Nonetheless, the task of measuring transport and how this varies over time poses a significant challenge due to its interactions with the surrounding waters such that the instantaneous transport will include not only the ocean- or gyre-scale "throughput" of interest, but also the large and variable contribution from local recirculations induced by

1. Graduate School of Oceanography, University of Rhode Island, Narragansett, Rhode Island, 02882, U.S.A.
2. Corrresponding author. ***email: trossby@gso.uri.edu***
3. School of Marine and Atmospheric Sciences, State University of New York, Stony Brook, New York, 11794, U.S.A.

the constant shifting in position, direction of flow and curvature of the current in addition to the often present GS rings. The other practical challenge is that of identifying the edges of the current because unless correctly identified, the estimated transport will inevitably be biased downward from its true value, particularly on the cyclonic side where the lateral shear at zero velocity often is quite large. The large short-term variability of the current coupled with infrequent sampling can make it difficult to separate out or distinguish the longer-term variations. Given the GS's prominence in the large-scale wind-driven and meridional overturning circulation, it behooves us to measure its transport accurately and confidently.

The above challenges notwithstanding, our knowledge of GS transport has improved significantly over the years. This results from a growing database on the one hand and improved methodologies on the other. Since the 1930's well over 100 hydrographic sections have been taken downstream of Cape Hatteras (see Iselin, 1940; Worthington, 1976; Sato and Rossby, 1995 (hereafter SR) for major compilations), and $O(10^3)$ acoustic Doppler current profiler (ADCP) sections in the last 17 years. In 2005 Rossby *et al.* (hereafter RFD) gave a first major compilation of transport measurements from the ADCP program. Since that time we have operated a deeper reaching ADCP enabling us to estimate directly vertical gradients of transport. In this paper we extend that earlier study to include all ADCP data through September 2009.

A very fortunate aspect of the New Jersey-Bermuda route is that it crosses the Gulf Stream where it exhibits a node in meandering (Cornillon, 1986). The route also spans the Slope and Sargasso Seas. The velocity data have been used in a wide range of studies, such as to examine the velocity and vorticity structure of the GS (Rossby and Zhang, 2001), cross-frontal exchanges as a source of nutrients (Schollaert *et al.,* 2004), the structure and variability of the outer shelf and slope currents (Flagg *et al.,* 2006), and spectral analyses of the horizontal velocity and near-surface temperature field (Wang *et al.,* 2010). The project was established primarily to gain a better handle on the GS and its variability. This paper reports on what we have found from the 17 years of operation, and puts these findings in perspective of other, earlier studies.

This paper differs from the above-mentioned RFD study in that we focus on the GS itself, not the surrounding waters. The analysis will confirm that by far most of the variability occurs on fast time scales, so fast that they cannot be resolved even with weekly sampling. This lack of sufficiently frequent, regular and complete sampling prevents a formal spectral analysis; nonetheless, the number of resolved crossings of the GS allows us to improve our knowledge of its variability on seasonal to interannual time scales. We also include a dynamical analysis of the 1873 Challenger section across the GS, ½-century before the start of repeat surveys of the GS. In the next section we briefly summarize the data and methods of analysis used here. The section thereafter presents the results. This is followed by a discussion of the principal findings and a brief summary.

2. Data and methods

The ADCP data comprise two subsets, data obtained with the 150 kHz ADCP that operated between fall 1992 and fall 2004, and 75 kHz data collection that began in 2005. Velocity is derived from the Doppler shift of the backscattered signal. In order to achieve maximum depth range, we sacrifice some detail such that the vertical resolution of the velocity profiles is 16 m. Operation has been effectively continuous since the start of the program, but for a variety of reasons the data return is far from uniformly distributed. The weekly roundtrip between Bermuda and New Jersey defines in principle a shortest resolvable period of one week. However, data from the northbound leg to New Jersey are often poor to nonexistent due to the light load factor and bow-up trim of the Oleander leading to greater downdraft of bubbles under the vessel. The southbound legs provide much better data return, but they too require reasonably good weather. Further, change in weather often results in only partial coverage of a transect. The strong temperature contrast across the "North Wall" of the GS can lead to shifty winds and concomitant spotty data returns in that area. Thus, we have less data to work with in winter, and gaps can occur at any time. We endeavor to process the data on a weekly schedule. This allows us to respond to problems quickly; nevertheless there are a couple of cases with downtimes of order 3 months due to equipment failures. Finally, it took us several months to overcome a bug with the new 75 kHz ADCP and we were not able to save data for depths greater than 400 m for seven months in 2005.

The velocity measurement has typically 1–2 cm s^{-1} accuracy, but this cannot be guaranteed at all times because it depends not only on the instrument itself but also on continuously accurate knowledge of vessel speed and heading. The latter is obtained from a Thales ADU5 3D-GPS. Although its overall performance is quite good, drop-outs do occur at which time we depend upon the vessel's gyrocompass (calibrated from recent prior and later ADU5 input). The main cause of dropouts seems in retrospect to be intermittency caused by weathering and gradual aging of the four antennae and cables. We do not know of any significant bias that could contaminate the resulting estimates of absolute velocity. One measure of the absence of bias is that the grand average of transport estimated from all southbound transits (N = 408) agrees with the northbound set (N = 187) to within 1.3%. Transport is very sensitive to heading errors so this gives us confidence in the installation and calibration procedures. Thus we make no distinction between directions of travel in the following analyses. The 150 kHz instrument had limited depth reach, 200–300 m, in the GS. The 75 kHz instrument often reaches at least twice as deep. The reader is referred to Flagg *et al.* (1998) for further details about the ADCP installation and operation on the MV Oleander.

The method of transforming or rotating the observed velocity data into stream or natural coordinates follows past practice (e.g. Halkin and Rossby, 1985, hereafter HR; Johns *et al.,* 1995). In order for a transit to be included in the data set considered here we require a discernable velocity maximum within the latitude band 36.6–39.2°N (these limits chosen to distinguish between the GS and GS rings) and that within that band the largest data gaps

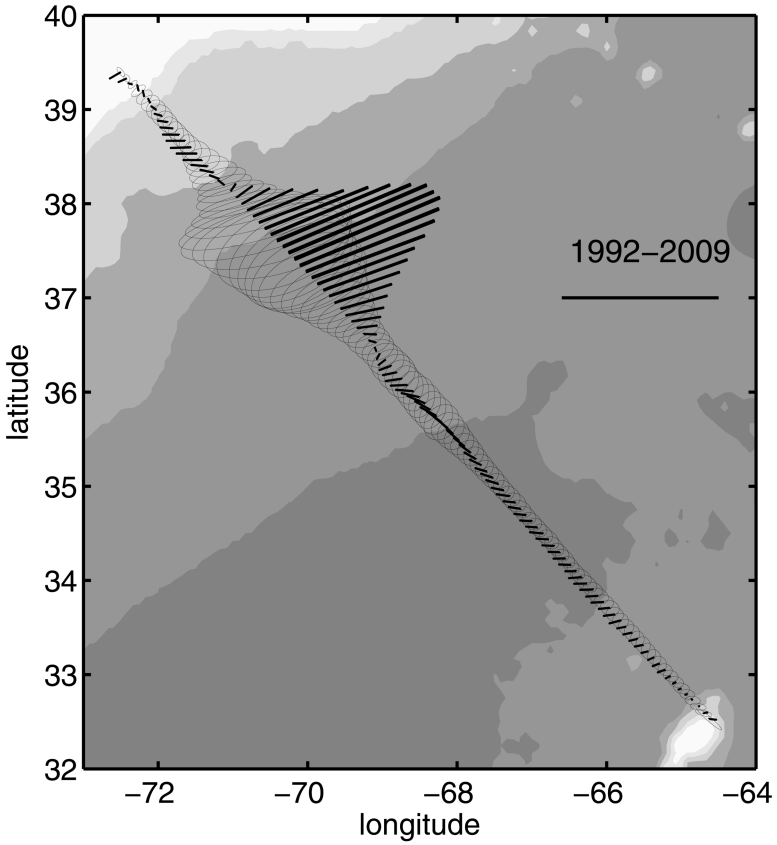

Figure 1. Mean velocity and variance ellipses between the mid-Atlantic Bight shelfbreak and Bermuda at 55-m depth for the 1992–2009 period. The bar corresponds to 1 m s^{-1} and 0.5 m^2 s^{-2}, respectively.

span less than 20 km, this to insure that the section is reasonably complete. In practice, a given section will have rather complete coverage or else some part, often near the North Wall, will be largely missing thus voiding its inclusion in these analyses. The peak velocity vector defines the position and direction of GS flow at that time.

3. Results

a. The mean field

i. The horizontal structure. The directly measured mean flow and variance ellipses of the GS at 52–55-m depth along the Oleander route are shown in Figure 1. This figure has changed hardly at all with the additional 2004–2009 data, but is included here for orientation. It shows a westward flow everywhere outside the GS, in both the Slope and Sargasso Seas. It also shows a distinct decrease in variance south of 35°N. Figure 2 shows

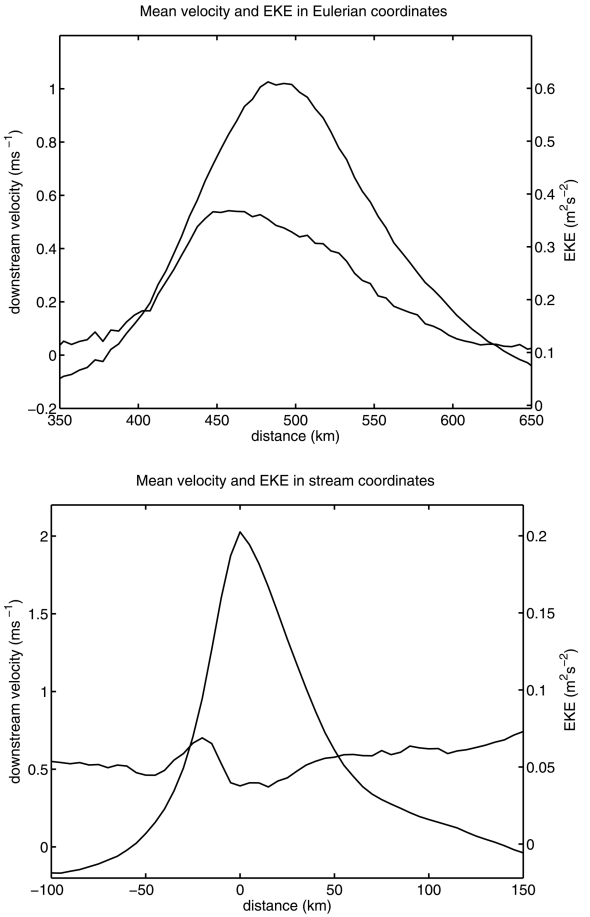

Figure 2. Mean downstream speed at 55-m depth (left axis) and corresponding variance (right axis) in Eulerian coordinates (top panel) and stream coordinates (bottom panel). The average layer transport between zero crossings = 1.29×10^5 m^2 s^{-1} (top panel) and 1.32×10^5 m^2 s^{-1} (bottom panel).

the mean flow and its variance in Eulerian or geographical coordinates (top panel), and in stream or natural coordinates (bottom panel). The abscissa indicates along-track distance from 40°45′N 74°W and distance from the center of the current, respectively (both in km). The roughly factor 8 reduction in variance from geographical to natural coordinates clearly demonstrates that most of the Eulerian variability observed in the GS results from the meandering of the current and not from structural changes to the current itself. The coincidence of maximum variance with the region of cyclonic shear reinforces this point. Johns *et al.* (1995) make the same observation of the GS farther east where the envelope of meandering is rapidly widening just west of the New England Seamount Chain. The lower panel indicates that although the current meanders through (and also induces) a highly

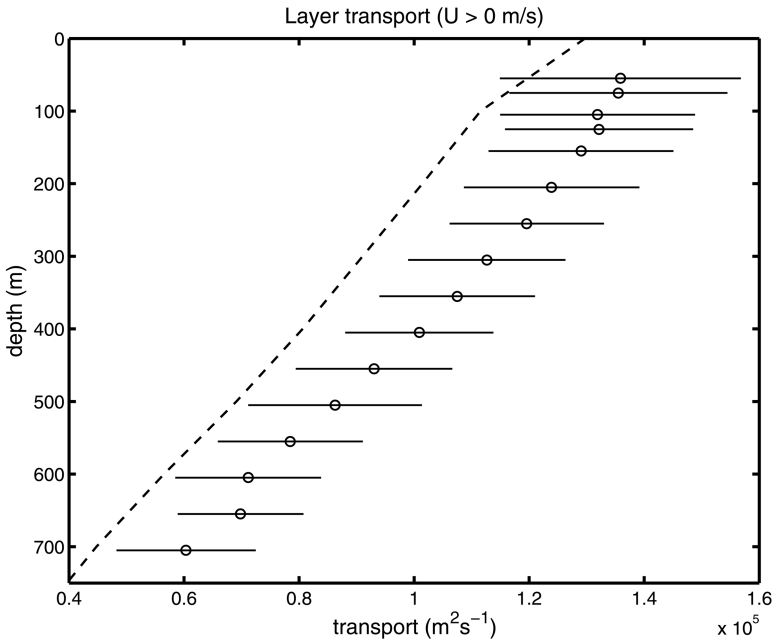

Figure 3. Mean and standard deviation of layer transport from 75 kHz ADCP (2005–2009) constructed from sections that deviate from the 23° (relative to east) mean direction of GS by no more than ±30°. The dashed line shows corresponding layer transport at the Pegasus line (HR).

variable environment, one can in fact average out this variability and obtain a well-defined mean flow given a large number of resolved sections. This has been shown in many studies (e.g. HR; Johns *et al.,* 1995; Rossby and Zhang, 2001).

ii. The vertical structure. The ADCP sections, frequent and accurate though they are, have the limitation of not reaching very deep raising the question of how well they represent the water column underneath. To examine this we use the recent 75 kHz data to construct a profile of mean of layer transport. This approach also enables us to compare directly a variety of sources including, in addition to ADCP data, the many hydrographic sections that have been accumulated over the years (SR), the Pegasus sections from the early 1980's (HR), and even moored current meter data that have been remapped into stream coordinates (Johns *et al.,* 1995). Here we update the RFD paper to include the recent 75 kHz data, which in the best of circumstances can reach as deep as 700–800 m.

Figure 3 profiles the mean and standard deviation of layer transport (1 m thick) between 55 and 705 m depth for the period 2005–2009. The integration across the current is defined by the first occurrence of zero downstream velocity to either side of the local velocity maximum. It also shows the corresponding profile from the 1980–1983 Pegasus program about 300 km upstream, closer to Cape Hatteras (HR). One can show (see Discussion) that

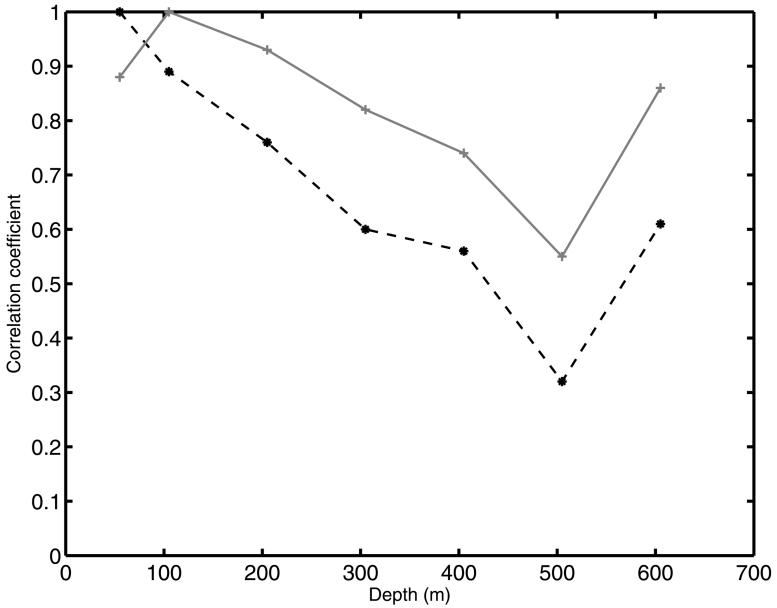

Figure 4. Correlation of layer flux as a function of depth with flux at 55 m (dashed line) and 105 m (gray line). The number of samples decreases from 95 for the top layers to 40 at 300- and 400-m depth to 27 and 14 for the deepest two layers. The correlations are significant at the 95% at all depths except at 505 m.

the difference agrees in magnitude with the relatively depth-independent inflow of water from both the Slope and Sargasso Sea side at the Pegasus line (HR).

The fluctuations in transport are quite coherent in the vertical. Figure 4 shows correlation of layer flux from the surface down, using either 55 or 105 m as a reference layer. The latter exhibits better correlation with the water column than does 55 m suggesting additional activity limited to the near-surface environment. The figure shows statistically significant correlation of transport down to the upper thermocline at 605 m although there is a curious drop in correlation at ~500-m depth. We return to this in the discussion.

b. Temporal patterns

We now examine the temporal variability of layer transport in different frequency bands. The unit of information for all that follows will be transport at 52 m (150 kHz ADCP until fall 2004) or 55 m (75 kHz ADCP thereafter), defined as the amount of water crossing the ship's track in the GS area with the limits of integration set by where the velocity normal to the ship's track (oriented along ~140° and ~320°) first goes to zero from either side of the downstream velocity maximum. Integration takes place in the form of trapezoidal summation with a maximum allowed (along-track) data gap of 20 km. The resulting time series exhibits considerable variability on short time scales. As noted earlier, these are

caused by the meandering of the current and induced nearby circulations. First, we estimate the annual cycle; this can be done quite well thanks to 17 years of sampling. We then look at inter-annual variations by averaging data into 12-month segments, stepped every 6 months.

i. The annual cycle. The simplest way to get a handle on the annual cycle is to overlay all data from the entire 1993–2009 period as a function of time of year only as shown in Figure 5, where the top and bottom panels represent transport at 55- and 205-m depth. The least squares sine fit to the data has an amplitude of 5900 $m^2\ s^{-1}$ or 4.3% of the mean flow at 55 m and 1787 $m^2\ s^{-1}$ or 1.5% of the mean flow at 205-m depth. These are quite small compared to the 16 and 14% scatter for the two layers. The volume of data decreases rapidly with a further increase in depth precluding reliable estimates of the annual cycle at greater depths. Note also the lower data return in winter. Together, these two panels strongly suggest that the annual cycle has a surface intensified signal.

ii. Interannual variations. To look at the longer time scales we bin the data in yearly segments stepped every ½-year, Figure 6. The unequal spacing of the data reflects the averaging in both magnitude and time. A 4-point running boxcar average of these leads to the dashed line. The standard deviation of the two lines relative to the mean is 5 and 3.2%, respectively. The boxcar has a half-power point at about twice its length or about 4 years. While the variance at these long time scales may not be very large, significant changes can develop on time scales of a few years, such as at the very start of the time series and during the 2000's with a maximum in 2004 and minimum in 2007, a range of 12% of the mean. A linear least square fit indicates a less than 1% increase during this 17-year period.

4. Discussion

The Oleander space-time series is the longest running ADCP operation of ocean current measurements. The single most important and considerable strength of this project lies in the very large set of high resolution horizontal transects enabling us to delineate the instantaneous location of the GS, and thereby quantify the uncertainty inherent in a single estimate of transport on the one hand, and through appropriate averaging determine (i) the annual cycle, and (ii) longer term variations.

Earlier hydrographic studies of GS transport (Worthington, 1976; SR) noted the large uncertainty in estimating transport due to the large scatter between sections. The same observation obtains here. While direct measurement of currents still has limited depth capability, we find that the average scatter around 1-year means for the 17-year period is 15%. This appears to be quite similar in magnitude to that of the SR study, which in their Figure 10 shows ~10 Sv (1 Sverdrup = $10^6\ m^3\ s^{-1}$) deviation around a 71 Sv mean baroclinic transport. These studies agree that what might be called the inherent uncertainty in estimating mean transport from a single section across the GS is about 15%.

The 75 kHz ADCP allows us to profile layer transport to greater depths than in the past

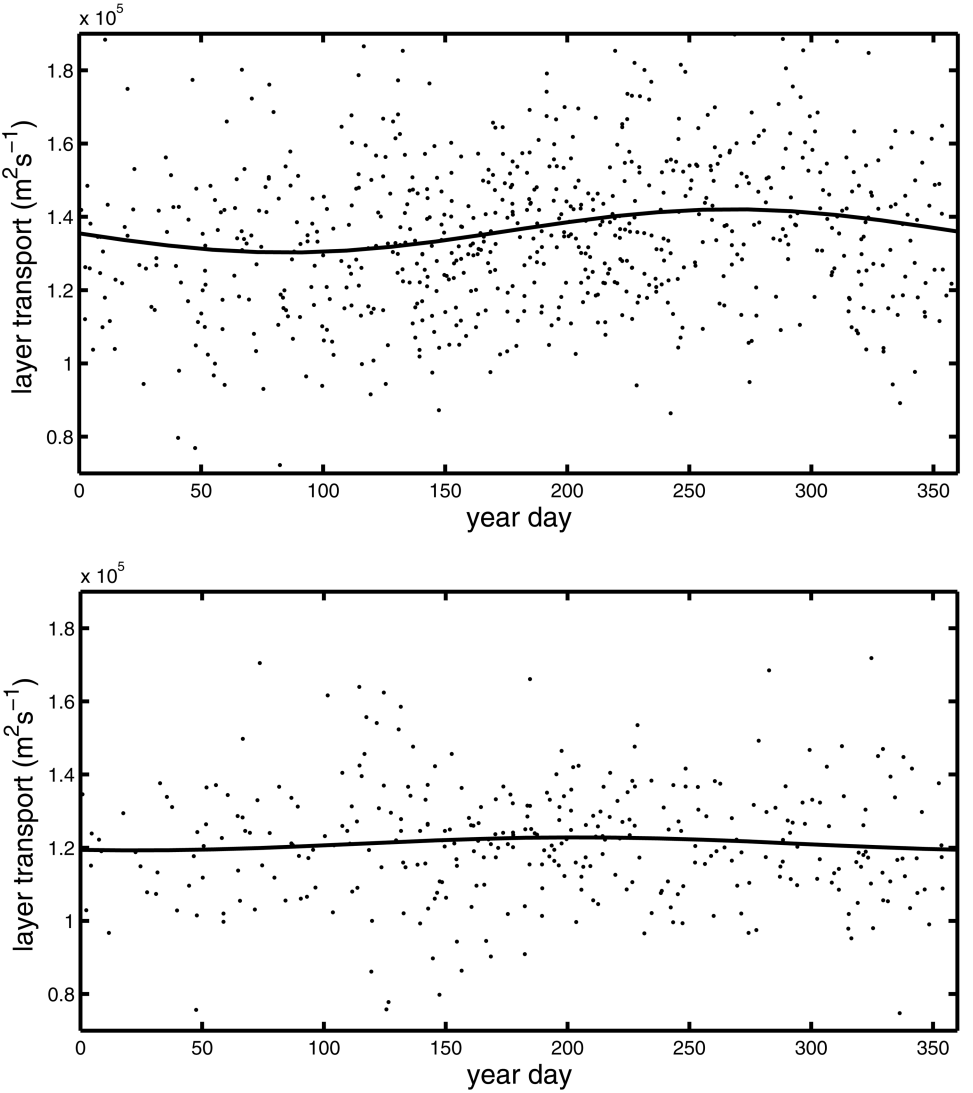

Figure 5. Annual cycle of layer transport at 55- and 205-m depth (top and bottom panels). The amplitudes of the sine fit as a fraction of their respective means are 4.6 and 1.8%. They are significant at the 99% (N = 400) and 88% (N = 250) levels, respectively. The scatter of the data around the respective fits is 16% and 14%.

(Fig. 3). Although the data for the figure come from the last five years only, they reveal clearly the expected baroclinic shear in transport. An almost identical rate of decrease in layer transport can be seen in the 1980–1983 Pegasus program at 73°W (HR), dashed line in Figure 3, The offset may be explained in terms of the strong inflows from both sides at

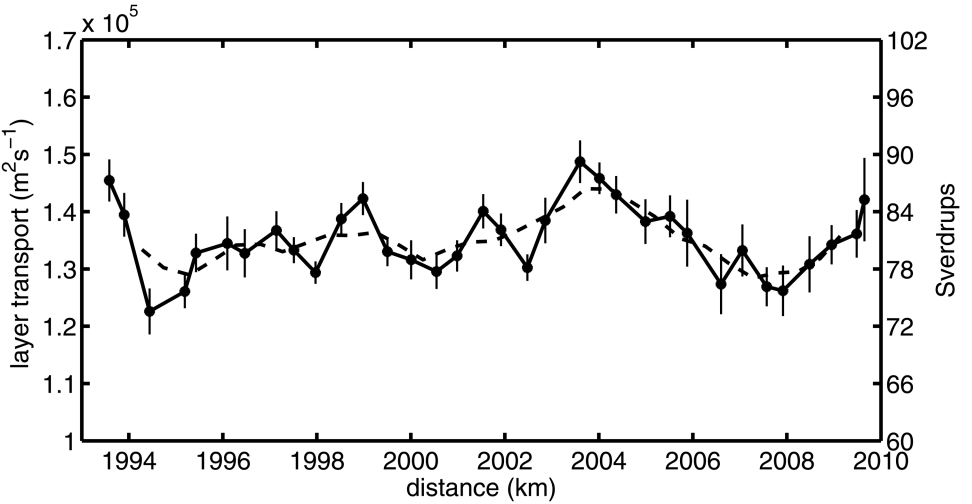

Figure 6. Low-pass filtered layer flux. Solid line = 1-year averages stepped every 6 months. Dashed line = 4-point running average of solid line. The vertical bars indicate standard error. The right-hand axis indicates transport variations using a scale factor of 600.

the Pegasus line. HR reported weakly depth-dependent inflow from both sides of about 0.06 m/s, somewhat less at depth reflecting the entrainment of Slope and Sargasso Sea water. The nearly depth-independent offset of 0.2×10^5 m^2 s^{-1} in Figure 3 between the Pegasus and Oleander lines, separated by about 300 km, could be accounted for with an average inflow of 0.2×10^5 m^2 s$^{-1}/3 \times 10^5$ m $= 0.07$ m s^{-1}, i.e. of the right magnitude. However, at the Oleander line there is a conspicuous outflow to the north of almost 0.1 m s^{-1} and almost nothing to the south (Rossby and Zhang, 2001) indicating that the mean in- and outflows possess considerable along-stream "finestructure" that would appear to preclude a detailed accounting for the differences in layer transport between the two lines.

While the scatter in layer transport applies to the upper ocean only, Figure 4 shows high correlation of velocity between 600 m and the top 100 m. This agrees with other studies that show that the vertical structure of flow in the GS can be accounted for quite effectively with only a few flat-bottom linear dynamical modes (e.g. Rossby, 1987). More generally, the highly coherent tilt of the density field across the GS explicitly requires a correspondingly high coherence to the baroclinic flow field. Hence variability of the near-surface waters will be representative of the baroclinic water column. But it is curious that the correlation drops at depths around 500 m. Given the limited amount of data this could be a fluke, but it could also point to some embedded layer-limited activity such as lenses, in which case they very likely would be layered in or organized by the density field. The significance of this low correlation may become clearer as the database grows.

The amplitude and phase of the sine wave estimate of the annual cycle at 55-m depth shows a clear maximum in mid-September with amplitude of 5900 m^2 s^{-1} (equivalent to a

0.03 m s^{-1} speed for a 200-km wide current). It decreases to 1787 m^2 s^{-1} at 205-m depth. It is unclear at this stage what happens at greater depths due to insufficient data. If this annual cycle is viewed as a strictly surface-limited signal superimposed on a seasonal modulation of the main baroclinic current, i.e. one that drops *linearly* to 0 at 205-m depth, say, we would obtain a seasonal thermocline transport cycle with an amplitude of (5900–1787) m^2 s^{-1} × 205 m × ½ = 0.4 Sv (as if 5900 had been measured at the surface). The seasonal modulation of the GS transport would be roughly 1787 m^2 s^{-1} × 600 ~ 1.1 Sv, where the factor 600 can be understood as the equivalent thickness of the upper layer of a 2-layer GS-system (see Appendix A for further details). These numbers (0.4 Sv and 1.1 Sv) can be compared to the corresponding baroclinic estimates in the SR study: 0.3 Sv and 4 Sv amplitude assuming 0 velocity at 300 and 2000 m, respectively. The agreement for the surface layer is reasonably good. On the one hand the seasonal cycle decays more rapidly than linearly with depth as assumed here; this would reduce our estimate. Unfortunately, the lack of data from the crucial top 50 m where the seasonal amplitude is largest makes a more detailed assessment problematic. Nonetheless, these findings are encouraging, especially in light of the close agreement with SR in phase, a maximum in September. With regard to the water column, the SR hydrographic estimate should more reliable. It is an integral in the vertical compared to a single layer estimate at 205-m depth. The question of why the seasonal amplitude is so small here warrants further study: does the scale factor 600 used above for steady flow apply to a seasonal cycle? In addition, we have no idea if there exists a barotropic component, and if so what would be its amplitude and phase. It is noteworthy that the seasonal cycle at 205-m depth has its maximum in July, close to that of the SR study. A recent paper by Beal *et al.* (2008) reports that the seasonal signal in the Florida Straits peaks slightly earlier (May–June–July) with a range (twice the amplitude) of 4.7 Sv, larger than what we estimate from the 205 m signal and smaller than the SR amplitude.

The long time series of directly measured transport gives us a more detailed view of the structure of interannual variations than has been possible in the past. Thus, a dramatic drop at the very start of the measurement program, then a 10-year period of gradual increase with ~2–3 year fluctuations before a 12% drop over 3–4 years, since then back to average values in 2009. RFD comment at some length on the first event, noting that it showed up in both the Bermuda hydrographic time series as well as in the Florida Straits transport record (see DiNezio *et al.,* 2009). These swings, when multiplied by 600 to estimate the corresponding baroclinic transport, amount to a 10 Sv range in flux variations and thus in absolute terms are significantly larger than those observed on these time scales in the Florida Straits (DiNezio *et al.,* 2009). Nonetheless, it seems highly plausible that Florida Straits variations do contribute to variability at the Oleander transect, but given that baroclinic transport at the Oleander line is well over twice as large, one should look elsewhere for additional sources of transport variability.

An obvious question would be whether transport variations in the GS correlate with flux variations in the surrounding waters. Figure 7, an update of Figure 5 in RFD shows the total

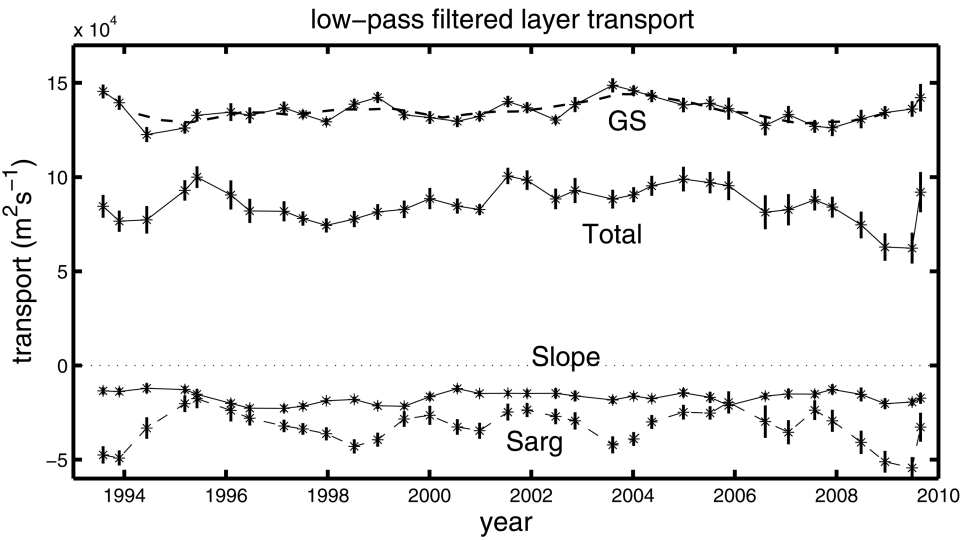

Figure 7. The five curves from top to bottom show 1-year averages stepped every 6 months for the Gulf Stream (dashed line from previous figure), total flux between the continental shelf edge and Bermuda (= sum of other 3 curves), the Slope Sea, and the Sargasso Sea (dashed line).

net flow at 55-m depth between the continental shelf break and Bermuda and its three subregions: the GS flow east (positive) and the Slope and Sargasso Sea fluxes, both flowing west across the Oleander line (negative). Slope Sea flow exhibits only small and slowly varying flows. The Sargasso Sea, on the other hand evinces quite large and rapid fluctuations, but its potential relationship to the GS needs further study.

The GS shows what appears to be a significant correlation with the NAO-index (http://www.cpc.noaa.gov/data/teledoc/nao.shtml). In Figure 8 we plot the 1-year low-passed filtered NAO-index in the top panel, and the GS flux (from Fig. 7) in panel b. The GS has a correlation coefficient of about -0.4 at 3–5 month lag with respect to the NAO-index and appears to be significant at the 90% level. It is thanks to the length of the time series (a major objective of the Oleander program) that these patterns appear to be emerging. The negative correlation means that its layer transport decreases for positive NAO values. A positive NAO index means that the westerlies in the Gulf Stream area are weaker than normal, and vice versa for a negative NAO index (see Figure 5a in DiNezio *et al.,* 2009). One possibility might be that weaker winds mean a weaker Ekman flow and convergence to the south leading to a lessening of sea level slope with a corresponding reduction in near-surface transport. The bottom panel shows the position of the GS (as measured by the location of the maximum velocity vector). It shifts northward with a slight delay when the NAO index is positive. This has been noted in many studies (e.g. Joyce *et al.,* 2000; Rossby and Benway, 2000; Hameed and Piontkovski, 2004).

It is appropriate here to recall the work by Sturges and Hong (2001), who argued that

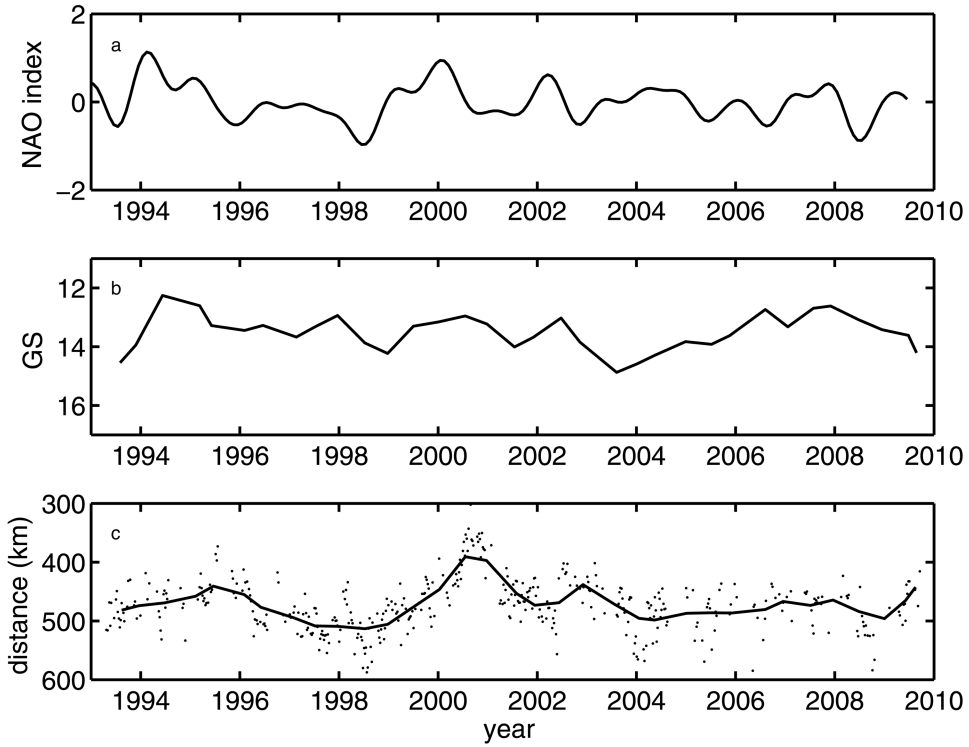

Figure 8. The three panels show: (a) NAO index, (b) GS layer flux/10^4 (note reversed y-axis), (c) and position of maximum velocity vector in km from 40.75°N 74°W along the Oleander line. The monthly NAO index has been filtered with a 1-year low-pass filter. Panel (b) is as in Figure 7; the line in (c) is a 1-year average of all data stepped every 6 months.

interannual variations in GS transport off the U.S. east coast have a wind-driven origin. In fact, they were able to account for much of the interpentadal variability in the hydrographic record reported by SR. This points to winds as a major driver of GS variations on these time scales. If, in fact, winds do account for most of the interpentadal transport variability, it must follow that the MOC (i.e. the thermohaline) contribution to GS transport has been quite stable over the 80 years of direct measurement since the upper or north-flowing limb of the MOC must pass through the Oleander section. By stable we mean a lack of any secular trend on multi-decadal time scales. There is even suggestive evidence of stable transport over the last 140 years based upon a H.M.S Challenger section.

On May 1, 1873 the H.M.S. Challenger crossed the GS while conducting a survey from Bermuda toward New Jersey. So far as we know this is the first hydrographic crossing of the GS. Seven temperature profiles were taken, the first one just off Bermuda and the last one in the slope waters just north of the GS, and only one within the current itself, Figure 9. We have used this section to estimate GS transport at the time. This can be done quite

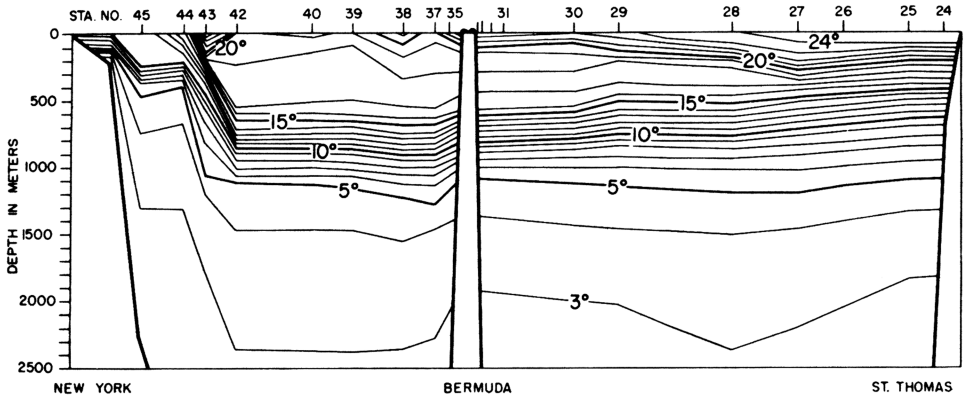

Figure 9. The 1873 temperature section between the Virgin Islands, Bermuda and New York (Thompson, 1877).

accurately because geostrophic transport depends only upon the difference in potential energy anomaly (PEA) bracketing the flow of interest (Fofonoff, 1962). We consider the PEA difference between Challenger stations 42 and 44. To do this, we examine a large number of modern stations (from the SR study) to either side of the GS to establish a regression between PEA and average temperature for a selected depth range across the thermocline. Given average temperature from these stations we then have the local PEA, from which transport is obtained. See Appendix B for further details. The result is shown in Figure 10. That the estimated transport should fall right on the SR annual cycle of transport is, of course, a coincidence given the 15% measurement uncertainty established above, but it does suggest that an average transport a century earlier might have been close to what we observe today.

5. Summary

This paper provides an updated overview of the longest time scales of variability in the GS off the U.S. east coast. Seventeen years of directly measured upper-ocean currents show that the average scatter of single transport estimates around 1-year means is about 15%, an estimate that fits with the scatter seen in earlier hydrographic estimates of transport. The annual cycle of layer transport is strongly surface-intensified with an amplitude of 4.3% at 55-m depth with a maximum in September. At 205 m the amplitude has decreased to a third. The surface-forced seasonal cycle should be significantly damped at this depth such that the remaining seasonal signal should be seen as a modulation of GS transport. While the seasonal cycle of surface transport agrees reasonably well with hydrographic estimates (SR), our direct estimate of the seasonal modulation of the GS is smaller than that of SR by a factor 4. Most likely this reflects (i) an uncertainly in how to scale up this layer estimate to encompass the entire GS, and (ii) a complete lack of knowledge about seasonal variations of the deep barotropic component. Clearly, we need

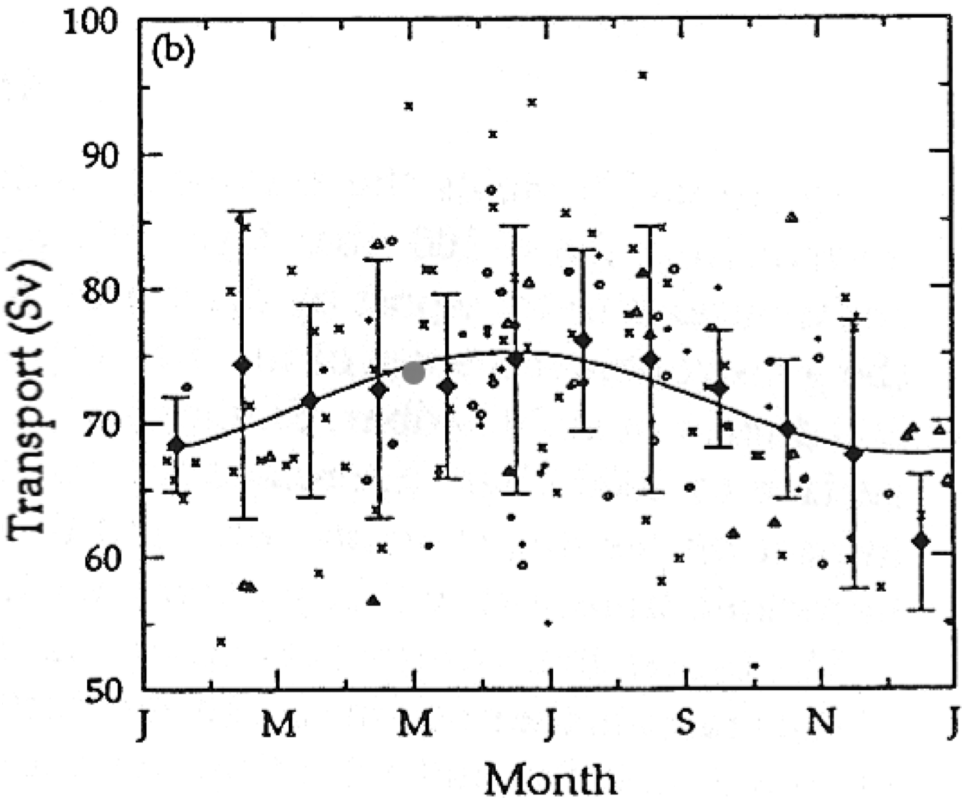

Figure 10. Baroclinic transport (0–2000 dbars) from SR (Fig. 7) with the Challenger estimate superimposed (large dot in May).

to measure currents to greater depths. Annually averaged variations in transport at 55-m depth have a standard deviation of 5% for the 17-year record. This drops to 3.2% for periods of two years and longer. There is clear evidence of a correlation between the NAO and GS such that its transport weakens when the NAO is in a positive phase. This result together with the Sturges and Hong (2001) study, which concluded that most of the observed interpentadal variability reported by SR can be accounted for in terms of time-varying winds over the North Atlantic, suggests that the upper branch of the MOC, the other component of GS transport, has been quite stable over the last 80 years.

Acknowledgments. Many have contributed to the Oleander project over the years. We are indebted to the Bermuda Container Line for their continued support of the ADCP operation onboard the Oleander. We particularly thank Ms. Sandy Fontana for her careful attention to all aspects of the data acquisition system and data processing. Mr. George Schwartze has been a central figure in maintaining the continual operation of the equipment onboard the Oleander. For the first five years the Oleander program was funded by NOAA; since then the activity has been supported by grants

from the NSF. ONR has also provided very helpful assistance. We thank two reviewers for their comments which helped improve the paper significantly.

APPENDIX A

The 12°C isotherm coincides rather closely with the surface of maximum stratification in the GS. It sits at about 900- and 300-m depth on the Sargasso and Slope Sea sides, respectively. The mean of these two is 600 m. This could be seen as the average depth of the thermocline in the GS. In somewhat more formal terms the surface transport is measured geostrophically by the difference across the GS of dynamic height anomaly, integrated from a reference pressure to the surface:

$$\Delta D = \int \delta dp$$

where δ is specific volume anomaly and p is pressure. The volume transport is measured by the difference potential energy anomaly across the GS of the (Fofonoff, 1962):

$$\chi = g^{-1} \int \delta p dp.$$

The integral differs from the dynamic height anomaly integral with the factor p inside, which measures from what depth the major contribution of δ comes from. δ increases rapidly from below across the main thermocline at 900 and 300 m for the Sargasso and Slope Sea sides, respectively, for an average of 600 m.

APPENDIX B

The H.M.S. Challenger crossed the GS May 1, 1873 during its transit from Bermuda toward New Jersey. The data are tabulated in the Challenger report (Tizard *et al.,* 1885). The units are °F and fathoms. The Miller-Casella thermometers were min-max thermometers with protected bulb. Although the Challenger expedition included extensive studies of seawater chemistry, concurrent water samples for salinity determinations were not taken. By modern standards the data have significant shortcomings—particularly for water mass analysis. But for several reasons these need not apply for estimating transport, especially given what we know today about the GS, and the application of the dynamic method. The first and principal reason is that estimating velocity as a function of depth depends only upon the *difference* in density structure between two points. Taking this one step further, if one wants total transport by the current, one needs only know the density profiles to either side, just outside the current. That is the remarkable beauty of the dynamic method. The second reason lies in the fact that density depends principally upon temperature so uncertainty in accuracy of salinity need not be a limitation. We further know that below about 11°C salinity has a very tight correlation with temperature across the entire current and even up to 18°C on the Sargasso Sea side (11°C is quite shallow on

the northern side) so it is only in the top ~200-m salinities exhibit large variability which includes a large seasonal component. We also surmise that the T/S-relationship has changed little over time. These factors greatly facilitate the estimation of baroclinic transport. But we can do better than this thanks to the well-defined structure of the density profile.

Meinen and Watts (2000) described a methodology for estimating the most probable temperature profile from the integral measurement of acoustic travel time from an inverted echo sounder on the ocean bottom. It owes its success to the fact that the temperature, salinity and density exhibit well-defined patterns of variability for a given location. By sorting profiles as a function of acoustic travel time, one will know with considerable accuracy the profile associated with a given travel time. This method, which now goes by the name of Gravest Empirical Mode (GEM), can use other observables as input to estimate the water column structure, one example being the depth of an isopycnal neutrally buoyant float (Perez-Brunius *et al.,* 2004). For the Challenger section we need to find the best estimate of density structure given knowledge of the upper ocean temperature structure. Experimenting with the large body of modern hydrographic data used in SR we found that an average temperature between 300 and 900 dbar south and 200 to 800 dbar north of the stream exhibited the strongest correlation with the density field. Finally, we note that to estimate transport we are interested in the vertical integral of the density profile.

To estimate baroclinic transport, we need the potential energy anomaly χ defined as

$$\chi = g^{-1} \int_0^P \delta p dp \quad [\mathrm{J\ m^{-2}}]$$

at two points bracketing the flow of interest, where p is pressure (from 0 to 2000 dbar) and δ is the specific volume anomaly (Fofonoff, 1962). For this purpose we have an excellent archive of 120 carefully reviewed GS sections (SR). We then correlate χ with average temperature for prescribed depth range north and south of the stream (depths are multiplied by 1.01 to approximate pressure in dbar). Given this correlation, the corresponding temperatures from the Challenger section will give us χ_2 to the south and χ_1 to the north. Baroclinic mass transport is then

$$M = \frac{\chi_2 - \chi_1}{f} \quad [\mathrm{kg\ s^{-1}}]$$

where f is the average Coriolis parameter (0.87×10^{-4} $\mathrm{s^{-1}}$). Dividing M by average density (1026.5 kg $\mathrm{m^{-3}}$) yields volume transport in Sv. Figure B.1 shows χ plotted against mean temperature between 300 and 900 m for the south side (top panel) and χ plotted against mean temperature between 200 and 800 m for the north side (bottom panel). Only stations for the months April–June have been used. Challenger stations 42 and 44 (Fig. 9) are closest to the stream without being in it. The mean temps for the two sides are 14.9 and

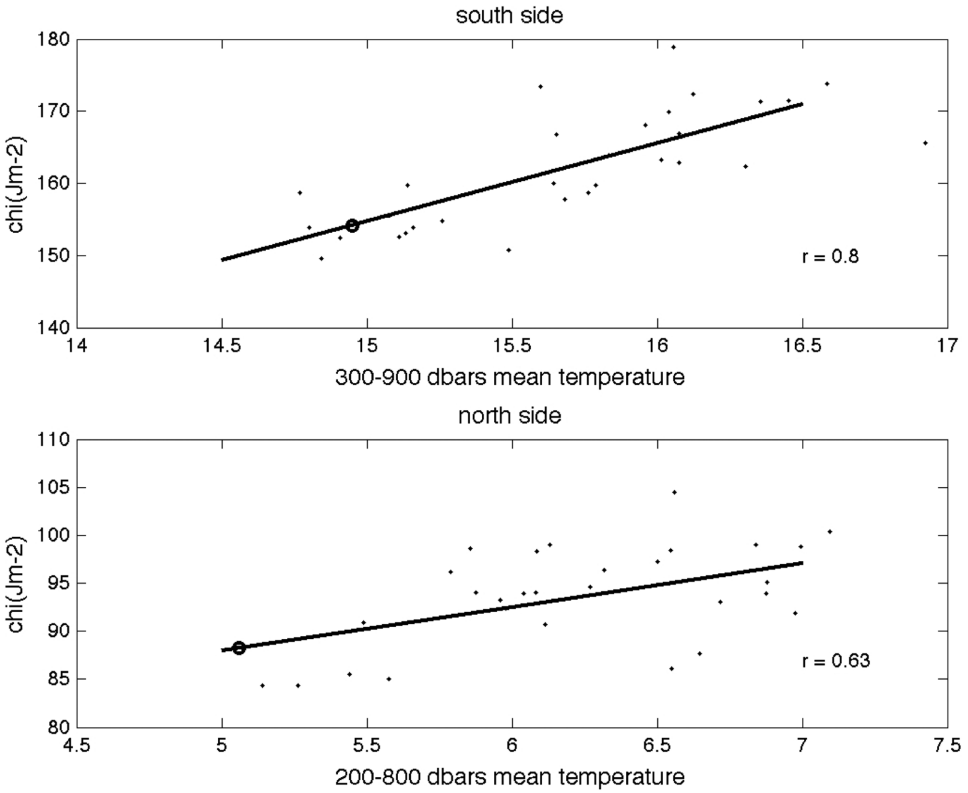

Figure B.1. PEA (0–2000 dbars) vs. mean temperature as indicated north (top panel) and south (bottom panel) for 31 hydrographic stations from the April–June months. The circle on the least square fit lines show the mean temperatures from Challenger stations 43 and 45.

5.0°C, respectively. Putting these into Figure B.1 yields χ values of 153.6 and 88 $\times$ 10^5 Jm^{-2}. These are also plotted in Figure B.2 using as reference Figure 6 in SR of PEA for the two sides. Although the values are low compared to the mean sinusoidal fit in the

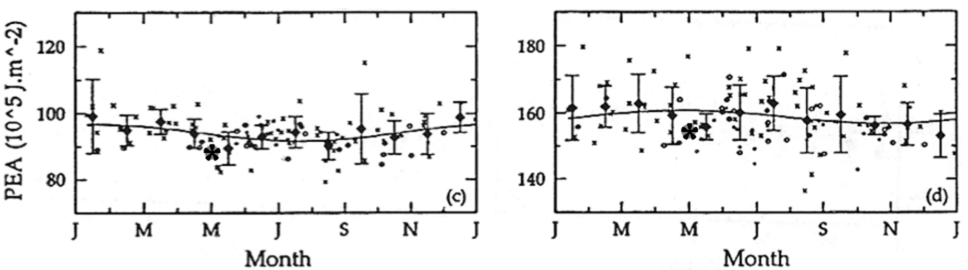

Figure B.2. PEA from Figure 6 in SR with the estimated PEAs north and south of the stream (large dots in May) as estimated from Figure B.1.

figure, they fall within the scatter of modern day observations. (A cursory inspection of SST trends for the last 150 years in the western Sargasso Sea suggests that temperatures may have been ~0.5°C lower at the time of the Challenger cruise. We know nothing about differences in the water column. The SST data were obtained from http://www.cru.uea.ac.uk/cru/data/temperature/.) The final step is to take their difference, divide by *f* and the average density and we obtain a volume transport of 73.5 Sv. This is plotted in Figure 10 using Figure 7 in SR.

Of course, we know little about the accuracy of the temperature profiles, in terms of both temperature and depth, but the greatest uncertainty may well be the ocean itself as noted earlier, not the measurements. The reason is the insensitivity of the differential estimate to instrument error. Suppose the thermometers all read 0.5°C too high (absolutely no reason to think this is the case), then the estimated transport would be only 3.9 Sv less. Similarly, if the depths were actually shallower by 5% (due to vertical shear acting on the lowered rope; pressure was not measured) the transport would be 5.6 Sv less. But again such a large error is highly unlikely because they were careful to steam to keep the line vertical (which had 150 to 200 kg as load for depth sounding).

REFERENCES

Beal, L. M., J. M. Hummon, E. Williams, O. B. Brown, W. Baringer and E. J. Kearns. 2008. Five years of Florida Current structure and transport from the Royal Caribbean Cruise Ship Explorer of the Seas. J. Geophys. Res., *113,* C06001, doi:10.1029/2007JC004154.

Cornillon, P. 1986. The effect of the New England Seamounts on the Gulf Stream meandering as observed from satellite IR imagery. J. Phys. Oceanogr., *16,* 386–389.

DiNezio, P. N., L. J. Gramer, W. E. Johns, C. Meinen and M. O. Baringer. 2009. Observed interannual variability of the Florida Current: Wind forcing and the North Atlantic oscillation. J. Phys. Oceanogr., *39,* 721–736, doi:10.1175/2008JPO4001.1.

Flagg, C. N., M. Dunn, D. Wang, H. T. Rossby and R. L. Benway. 2006. A study of the currents of the outer shelf and upper slope from a decade of shipboard ADCP observations in the Middle Atlantic Bight. J. Geophys. Res., *111,* C06003, doi:10.1029/2005JC003116.

Flagg, C., G. Schwartze, E. Gottlieb and T. Rossby. 1998. Operating an acoustic Doppler current profiler (ADCP) aboard a container vessel. J. Atmos. Ocean. Tech., *15,* 257–271.

Fofonoff, N. P. 1962. Dynamics of ocean currents, *in* The Sea: Ideas and Observations on Progress in the Study of the Seas, Vol. 1, Physical Oceanography, M. N. Hill, ed., John Wiley & Sons, 325–395.

Halkin, D., T. A. Rago and T. Rossby. 1985. Data Report of the Pegasus Program at 73°W, *85–2,* University of Rhode Island.

Halkin, D. and H. T. Rossby. 1985. The structure and transport of the Gulf Stream at 73°W. J. Phys. Oceanogr., *15,* 1439–1452.

Hameed, S. and S. Piontkovski. 2004. The dominant influence of the Icelandic low on the position of the Gulf Stream north wall. Geophys. Res. Lett., *31,* L09303, doi:10.1029/2004GL019561.

Iselin, C. O'D. 1940. Preliminary report on long-period variations in the transport of the Gulf Stream system. Papers in Phys. Oceanogr. Meteor., *VIII(1),* 40 pp.

Johns, W. E., T. J. Shay, J. M. Bane and D. R. Watts. 1995. Gulf Stream structure, transport and recirculation near 68°W. J. Geophys. Res., *100,* 817–838.

Joyce, T. M., C. Deser and M. A. Spall. 2000. The relation between decadal variability of subtropical mode water and the North Atlantic oscillation. J. Climate, *13,* 2550–2569.

Meinen, C. S. and D. R. Watts. 2000. Vertical structure and transport on a transect across the North Atlantic Current near 42°N: Time series and mean. J. Geophys. Res., *105,* 21,869–21,891.

Perez-Brunius, P., T. Rossby and D. R. Watts. 2004. A method to obtain the mean transports of ocean currents by combining isopycnal float data with historical hydrography. J. Atmos. Oceanic Tech., *21,* 298–316.

Rossby, T. and R. Benway. 2000. Slow variations in mean path of the Gulf Stream east of Cape Hatteras. Geophys. Res. Lett., *27,* 117–120.

Rossby, T., C. Flagg and K. Donohue. 2005. Interannual variations in upper ocean transport by the Gulf Stream and adjacent waters between New Jersey and Bermuda. J. Mar. Res., *63,* 203–226.

Rossby, T. and E. Gottlieb. 1998. The Oleander Project: Monitoring the variability of the Gulf Stream and adjacent waters between New Jersey and Bermuda. Bull. Amer. Met. Soc., *79,* 5–18.

Rossby, T. and H. M. Zhang. 2001. The near-surface velocity and potential vorticity structure of the Gulf Stream. J. Mar. Res., *59,* 949–975.

Sato, O. and T. Rossby. 1995. Seasonal and secular variations in dynamic height anomaly and transport of the Gulf Stream. Deep Sea Res., *42,* 149–164.

Schollaert, S. E., T. Rossby and J. A. Yoder. 2004. Gulf Stream cross-frontal exchange: possible mechanisms to explain interannual variations in phytoplankton chlorophyll in the Slope Sea during the SeaWiFs Years. Deep-Sea Res II, *51(1–3),* 173–188.

Sturges, W. and B. G. Hong. 2001. Gulf Stream transport variability at periods of decades. J. Phys. Oceanogr., *31,* 324–332.

Thompson, C. W. 1877. The voyage of the Challenger. The Atlantic, 2. MacMillan, London, 396 pp.

Tizard, T. H., H. N. Mosely, J. Y. Buchanan and J. Murray. 1885. Report on the Scientific Results of the Voyage of H.M.S. Challenger during the years 1873–1876. Narrative of the Cruise of H.M.S. Challenger with a General Account of the Scientific Results of the Expedition, 1, First Part, 1–510.

Wang, D.-P., C. N. Flagg, K. Donohue and T. Rossby. 2010. Wavenumber spectrum in the Gulf Stream from shipboard ADCP observations and comparison with altimetry measurements. J. Phys. Oceanogr., *40,* doi:10.1175/2009JPO4330.1.

Worthington, L. V. 1976. On the North Atlantic Circulation, Johns Hopkins Oceanographic Studies, *6,* 110 pp.

Received: *5 February, 2010;* revised: *24 July, 2010.*